# Strangeness magnetic form factor of the proton in the extended chiral quark model

C. S. An[1,*] and B. Saghai[2,†]

[1]*Institute of High Energy Physics and Theoretical Physics Center for Science Facilities, CAS, Beijing 100049, China*

[2]*Institut de Recherche sur les lois Fondamentales de l'Univers, Irfu/SPhN, CEA/Saclay, F-91191 Gif-sur-Yvette, France*

(Received 8 June 2013; revised manuscript received 21 July 2013; published 20 August 2013)

**Background:** Unravelling the role played by nonvalence flavors in baryons is crucial in deepening our comprehension of QCD. The strange quark, a component of the higher Fock states in baryons, is an appropriate tool to study nonperturbative mechanisms due to the pure sea quark.

**Purpose:** Study the magnitude and the sign of the strangeness magnetic moment $\mu_s$ and the magnetic form factor ($G_M^s$) of the proton.

**Methods:** Within an extended chiral constituent quark model, we investigate contributions from all possible five-quark components to $\mu_s$ and $G_M^s(Q^2)$ in the four-vector momentum range $Q^2 \leqslant 1\,(\mathrm{GeV}/c)^2$. The probability of the strangeness component in the proton wave function is calculated employing the $^3P_0$ model.

**Results:** Predictions are obtained by using input parameters taken from the literature. The observables $\mu_s$ and $G_M^s(Q^2)$ are found to be small and negative, consistent with the lattice-QCD findings as well as with the latest data released by the PVA4 and HAPPEX Collaborations.

**Conclusions:** Due to sizable cancellations among different configurations contributing to the strangeness magnetic moment of the proton, it is indispensable to (i) take into account all relevant five-quark components and include both diagonal and nondiagonal terms, (ii) handle with care the oscillator harmonic parameter $\omega_5$ and the $s\bar{s}$ component probability.

DOI: 10.1103/PhysRevC.88.025206 PACS number(s): 12.39.−x, 13.40.Em, 14.20.Dh, 14.65.Bt

## I. INTRODUCTION

Parity-violating electron scattering process, extensively investigated for more than a decade, has been proven to offer a unique experimental opportunity in probing the contribution of the strangeness sea to the electromagnetic properties of the nucleon. During that period, results from four collaborations have been released in several publications (for recent reviews see Refs. [1,2]) with the latest ones for each of the collaborations being: SAMPLE (MIT-Bates) [3], PVA4 (MAMI) [4], G0 (JLab) [5], HAPPEX (JLab) [6]. Those experiments allowed extracting linear combinations of electric ($G_E^s$) and magnetic ($G_M^s$) strangeness form factors of the proton as a function of four-vector momentum transfer $Q^2$.

A general trend of the data published before 2009 was to produce rather small and positive values for $G_M^s(Q^2)$, especially in the range $(Q^2) \simeq 0.1$ to $0.5\ (\mathrm{GeV}/c)^2$; see, e.g., Table 1 in Ref. [7]. In this latter work a global analysis of world data of parity-violating electron scattering was performed for $Q^2 \lesssim 0.3\ (\mathrm{GeV}/c)^2$ and led to $\mu_s = 0.12 \pm 0.55 \pm 0.07$ nuclear magneton ($\mu_N$). Another low $Q^2$ global analysis [8] disfavored negative $G_M^s$, and still a third one [9], dedicated to the range $\simeq 0.5$ to $1.0\ (\mathrm{GeV}/c)^2$, produced two sets of solutions with opposite signs.

On the theoretical side, the strangeness contributions to the magnetic moment of the proton have also been intensively investigated. Few approaches have produced results close to the data, with positive sign, such as heavy baryon chiral perturbation theory [10,11], quenched chiral perturbation theory [12], chiral quark-soliton model [13], Skyrme model [14], and constituent quark models [15–17]. However, a large number of theoretical results predicted negative values, notably, meson cloud model [18,19], chiral quark model [20,21], and unquenched constituent quark model [22]. A remarkable issue is that the lattice-QCD approaches [23–27] have kept predicting a negative strangeness magnetic moment for the proton. Note that in various works prior to the advent of the first data, the general trend was predicting a negative sign for the strangeness magnetic moment of the proton $\mu_s$, as reviewed in Refs. [28,29].

In 2009, the PVA4 Collaboration [4], obtained for the first time a negative sign value $G_M^s(Q^2 = 0.22) = -0.14 \pm 0.11 \pm 0.11$; units are $(\mathrm{GeV}/c)^2$ for $Q^2$ and nuclear magnetons for $G_M^s$. More recently the HAPPEX Collaboration [6] reported a small but also negative sign at higher $Q^2$, namely, $G_M^s(Q^2 = 0.624) = -0.070 \pm 0.067\mu_N$.

The present work is motivated by interpreting the recent data [4,6] on $G_M^s(Q^2)$ within an extended chiral constituent quark model ($E\chi$CQM).

Our starting point was the idea put forward by Zou and Riska [30] according to which the strangeness magnetic moment of the proton could be explained by including five-quark Fock components in the proton wave function. They showed that a positive strangeness magnetic moment of the proton can rise from the $\bar{s}$ being in the ground state and the four-quark subsystem $uuds$ in the $P$ state, while $\bar{s}$ in the $P$ state and the four-quarks in their ground state would lead to a negative value for $\mu_s$. Then that approach was developed and extended to the strangeness contributions to spin of the proton [31], magnetic moments of baryons [16], electromagnetic and strong decays of baryon resonances [32–35]. The main outcome of those studies is that the higher Fock components

*ancs@ihep.ac.cn

†bijan.saghai@cea.fr

 

play important roles in describing the properties of baryons and their resonances.

However, in Ref. [30] only contributions from the diagonal matrix elements $\langle uuds\bar{s}|\hat{\mu}_s|uuds\bar{s}\rangle$ were included, while the nondiagonal transition between the three-quark and strangeness components of the proton $\langle uud|\hat{\mu}_s|uuds\bar{s}\rangle$ also contributes. In fact, the diagonal contributions are proportional to the probability of corresponding strangeness component $P_{s\bar{s}} \equiv A^2_{s\bar{s}}$, but the nondiagonal contributions are proportional to the product of probability amplitudes of three- and five-quark components $A_{3q}A_{s\bar{s}}$. Generally, the latter is more significant than the former, given that the proton is mainly composed of three-quark component. In Ref. [16], the nondiagonal contributions were taken into account, but on the one hand, only the lowest strangeness component, with the four-quark subsystem in the $P$ state was considered, and on the other hand, the probability amplitudes for strangeness components in the proton were treated as free parameters in order to obtain a positive value for $\mu_s$.

In the present work, the probability amplitudes, a crucial ingredient in the extended chiral constituent quark model, are calculated within the most commonly accepted $q\bar{q}$ pair creation mechanism, namely, the $^3P_0$ model. Then, the $q\bar{q}$ pair is created anywhere in space with the quantum numbers of the QCD vacuum $0^{++}$, corresponding to $^3P_0$ [36]. This model has been successfully applied to the decay of mesons and baryons [37,38], and has recently been employed to analyze the sea flavor content of the ground states of the $SU(3)$ octet baryons [39]. Note that in the $SU(3)$ symmetric case, the ratio of probabilities for five-quark components with strange and light quark-antiquark pairs is $1/2$ [16], while by taking into account the $SU(3)$ symmetry breaking effects, we determined [39] that ratio to be $P_{s\bar{s}}/(P_{u\bar{u}} + P_{d\bar{d}}) = 0.057/(0.098 + 0.216) \sim 0.18$ and putting $P_{s\bar{s}} \sim 6\%$.

Moreover, we calculate both diagonal and nondiagonal terms for all relevant five-quark configurations and removed contributions from the center-of-mass motion of the quark clusters, as emphasized recently [17]. Finally, we underline that all of the input parameters are taken consistently from the literature.

The present paper is organized as follows. In Sec. II, we present our theoretical framework, which includes the wave function and the strangeness magnetic moment of the proton within our extended constituent quark model. Our numerical results for the strangeness magnetic moment and form factor of the proton are reported in Sec. III, where we give the input parameters, discuss the role of various ingredients of our approach, and proceed to comparisons with findings by other authors. Finally, Sec. IV contains a summary and conclusions.

## II. THEORETICAL FRAMEWORK

In this section, we first briefly review the method to derive the wave function of the proton in the extended chiral constituent quark model (Sec. II A), and then present the formalism for the strangeness magnetic moment of the proton (Sec. II B).

### A. Wave function of the proton

In our extended chiral constituent quark model, the wave function of the proton can be expressed as

$$|\psi\rangle_p = \frac{1}{\sqrt{\mathcal{N}}}\left(|3q\rangle + \sum_{i,n_r,l} C_{in_rl}|5q, i, n_r, l\rangle\right). \quad (1)$$

The first term in Eq. (1) is just the conventional wave function for the proton with three light constituent quarks, which reads

$$|3q\rangle = \frac{1}{\sqrt{2}}[1^3]_C\phi_{000}(\vec{\xi}_1)\phi_{000}(\vec{\xi}_2)\left(\varphi^p_\lambda\chi_\lambda + \varphi^p_\rho\chi_\rho\right), \quad (2)$$

where $[1^3]_C$ denotes the $SU(3)$ color singlet, $\varphi^p_{\lambda(\rho)}$ the mixed symmetric flavor wave functions of the proton, and $\chi_{\lambda(\rho)}$ the mixed symmetric spin wave functions for configuration $[21]_S$ with spin $1/2$ for a three-quark system. And $\phi_{000}(\vec{\xi}_i)$ are the orbital wave functions with the quantum numbers $n_r, l, m$ denoted by corresponding subscripts; $\vec{\xi}_i$ are the Jacobi coordinates defined by

$$\vec{\xi}_1 = \frac{1}{\sqrt{2}}(\vec{r}_1 - \vec{r}_2); \quad \vec{\xi}_2 = \frac{1}{\sqrt{6}}(\vec{r}_1 + \vec{r}_2 - 2\vec{r}_3). \quad (3)$$

The second term in Eq. (1) is a sum over all possible five-quark Fock components with $q\bar{q}$ pairs; $q \equiv u, d, s$. $n_r$ and $l$ denote the inner radial and orbital quantum numbers, respectively. As discussed in Ref. [39], here we only consider the case for $n_r = 0$ and $l = 1$, since probabilities of higher radial excitations in the proton should be very small, and those of higher orbital excitations vanish. Different possible orbital-flavor-spin-color configurations of the four-quark subsystems in the five-quark system with $n_r = 0$ and $l = 1$ are numbered by $i$; $i = 1, \ldots, 17$. Finally, $C_{in_rl}/\sqrt{\mathcal{N}} \equiv A_{in_rl}$ represents the probability amplitude for the corresponding five-quark component, which can be calculated by

$$C_{in_rl} = \frac{\langle QQQ(Q\bar{Q}), i, n_r, l|\hat{T}|QQQ\rangle}{M_p - E_{in_rl}}, \quad (4)$$

where

$$\mathcal{N} \equiv 1 + \sum_{i=1}^{17}\mathcal{N}_i = 1 + \sum_{i=1}^{17} C^2_{in_rl}, \quad (5)$$

and $\hat{T}$ is a transition coupling operator of the $^3P_0$ model

$$\hat{T} = -\gamma\sum_j \mathcal{F}^{00}_{j,5}\mathcal{C}^{00}_{j,5}\mathcal{C}_{OFSC}\sum_m\langle 1, m; 1, -m|00\rangle \times \chi^{1,m}_{j,5}\mathcal{Y}^{1,-m}_{j,5}(\vec{p}_j - \vec{p}_5)b^\dagger(\vec{p}_j)d^\dagger(\vec{p}_5), \quad (6)$$

with $M_p$ the physical mass of the proton.

Wave functions of the five-quark components can be classified into two categories by four-quark subsystems being in their $S$ state

$$|5q, i, 0, 1\rangle = \sum_{abc}\sum_{s_z m m' s'_z} C^{\frac{1}{2}\frac{1}{2}}_{1s_z,jm}C^{jm}_{1m',\frac{1}{2}s'_z}C^{[1^4]}_{[31]_a[211]_a} \times C^{[31]_a}_{[F]_b[S]_c}[F]_b[S]_c[211]_{C,a}\bar{Y}_{1m'}\bar{\chi}_{s_{z'}} \times \Phi(\{\vec{\xi}_i\}), \quad (7)$$

and $P$ state

$$|5q,i,0,1\rangle = \sum_{abcde}\sum_{Ms'_z m s_z} C^{\frac{1}{2}\frac{1}{2}}_{JM,\frac{1}{2}s'_z} C^{JM}_{1m,Ss_z} C^{[1^4]}_{[31]_a[211]_a} \times C^{[31]_a}_{[31]_b[FS]_c} C^{[FS]_c}_{[F]_d[S]_e} [31]_{X,m}(b)[F]_d \times [S]_{s_z}(e)[211]_C(a)\bar{\chi}_{s'_z}\Phi(\{\vec{\xi}_i\}), \quad (8)$$

where the flavor, spin, color, and orbital wave functions of the four-quark subsystem are denoted by the Young patterns. The coefficients $C^{\frac{1}{2}\frac{1}{2}}_{1s_z,jm}$ and $C^{jm}_{1m',\frac{1}{2}s'_z}$ in Eq. (7), and $C^{\frac{1}{2}\frac{1}{2}}_{JM,\frac{1}{2}s'_z}$ and $C^{JM}_{1m,Ss_z}$ in Eq. (8) are Clebsch-Gordan coefficients for the angular momentum, and others are Clebsch-Gordan coefficients of $S_4$ permutation group. $\bar{Y}_{1m'}$ and $\bar{\chi}_{s_{z'}}$ represent the wave functions of the antiquark. $\vec{\xi}_i$ denote the Jacobi coordinates for a five-quark system, analogous to the ones in Eq. (3), and $\vec{\xi}_i$ are defined as

$$\vec{\xi}_i = \frac{1}{\sqrt{i+i^2}}\left(\sum_{j=1}^{i}\vec{r}_j - i\vec{r}_i\right), \quad i = 1,\ldots,4. \quad (9)$$

Finally, the energies of five-quark components with quantum numbers $n_r = 0$ and $l = 1$ in constituent quark model can be expressed as

$$E_{i,0,1} = E_0 + \delta^i_m + \langle H_{\rm hyp}\rangle_i, \quad (10)$$

where $E_0$ is a commonly shared energy of the 17 different five-quark configurations, $\delta^i_m$ the energy deviation caused by the $s\bar{s}$ pairs, and $\langle H_{\rm hyp}\rangle_i$ denote matrix elements of the quarks hyperfine interactions in the five-quark configurations. In this work, we employ the hyperfine interactions mediated by Goldstone-boson exchange [40],

$$H_h = -\sum_{i<j}\vec{\sigma}_i\cdot\vec{\sigma}_j\left[\sum_{a=1}^{3}V_\pi(r_{ij})\lambda^a_i\lambda^a_j + \sum_{a=4}^{7}V_K(r_{ij})\lambda^a_i\lambda^a_j + V_\eta(r_{ij})\lambda^8_i\lambda^8_j\right], \quad (11)$$

where $V_M$ are the corresponding strength of the $M(\equiv\pi, K, \eta)$ meson-exchange interactions, and $\lambda^a_{i(j)}$ the Gell-Mann matrices in $SU(3)$ color space.

Explicit matrix elements of $\hat{T}$ and the energies $E_{i,0,1}$ were derived in Ref. [39], here we employ those results for calculations of the probability amplitudes of the strangeness components in the proton.

### B. Strangeness magnetic moment of the proton

In our model, calculations of the strangeness magnetic moment of the proton can be divided into two parts, namely, the diagonal and nondiagonal contributions. The former can be defined as the matrix elements of the following operator in the strangeness components of the proton:

$$\hat{\mu}^D_s = \frac{M_p}{m_s}\sum_i \hat{S}_i(\hat{l}_{iz} + \hat{\sigma}_{iz}), \quad (12)$$

where $\hat{S}_i$ is an operator acting on the flavor space, with the eigenvalue $+1$ for a strange quark, $-1$ for an antistrange quark, and 0 for the light quarks. Note that the operator $\hat{\mu}^D_s$ is in unit of the nuclear magneton.

The nondiagonal contributions of the strangeness magnetic moment, which involve $s\bar{s}$ pair annihilations and creations, are obtained as matrix elements of the operator

$$\hat{\mu}^{ND}_s = 2M_p\sum_i \frac{\hat{S}_i}{2}\mathcal{C}_{OFSC}\vec{r}_i\times\hat{\sigma}_i, \quad (13)$$

where $\hat{\mu}^{ND}_s$ is also in unit of the nuclear magneton. $\mathcal{C}_{OFSC}$ is an operator to calculate the overlap between the orbital, flavor, spin, and color wave functions of the residual three-quark in the five-quark components after $s\bar{s}$ annihilation and the three-quark component of the proton.

As reported previously [39], among the seventeen possible different five-quark configurations, the probability amplitudes of 12 of them with $s\bar{s}$ pairs are nonzero in the proton. Those configurations can be classified in four categories (Table I) with respect the orbital and spin wave functions of the four-quark subsystem, namely, configurations with: (i) $[31]_X$ and $[22]_S$; (ii) $[31]_X$ and $[31]_S$; (iii) $[4]_X$ and $[22]_S$; (iv) $[4]_X$ and $[31]_S$. Contributions of these four different kinds of configurations are described below.

(i) $[31]_X$ and $[22]_S$: The total spin of the four-quark subsystem is 0, therefore the diagonal matrix elements $\langle\mu^D_s\rangle$ are only from contributions due to the four-quark orbital angular momentum and spin of the antiquark,

TABLE I. Diagonal ($\mu^D_s$) and nondiagonal ($\mu^{ND}_s$) contributions of different five-quark configurations to the strangeness magnetic moment of the proton. Notice that the full expressions are obtained by multiplying each term by $\frac{M_p}{m_s}P^i_{s\bar{s}}$ for $\mu^D_s$ and by $\frac{4M_p}{9\omega_5}15^{3/4}C_{35}A_{3q}A^i_{s\bar{s}}$ for $\mu^{ND}_s$. The last column gives the flavor-spin overlap factors.

| Category | Configurations | $\mu^D_s$ | $\mu^{ND}_s$ | $C^i_{FS}$ |
|---|---|---|---|---|
| (i) $[31]_X[22]_S$: | | | | |
| | $[31]_X[4]_{FS}[22]_F[22]_S$ | 1/2 | $2\sqrt{3}/3$ | $\sqrt{2}/4$ |
| | $[31]_X[31]_{FS}[211]_F[22]_S$ | 13/24 | $2\sqrt{3}/3$ | $\sqrt{2}/4$ |
| | $[31]_X[31]_{FS}[31]_F[22]_S$ | 13/24 | $2\sqrt{3}/3$ | $\sqrt{2}/4$ |
| (ii) $[31]_X[31]_S$: | | | | |
| | $[31]_X[4]_{FS}[31]_F[31]_S$ | $-1$ | $-2\sqrt{3}/3$ | 1/2 |
| | $[31]_X[31]_{FS}[211]_F[31]_S$ | $-1$ | $-2\sqrt{3}/3$ | 1/2 |
| | $[31]_X[31]_{FS}[22]_F[31]_S$ | $-1$ | $-2\sqrt{3}/3$ | $1/\sqrt{6}$ |
| | $[31]_X[31]_{FS}[31]_F[31]_S$ | $-1$ | 2/3 | $-\sqrt{3}/6$ |
| (iii) $[4]_X[22]_S$: | | | | |
| | $[4]_X[31]_{FS}[211]_F[22]_S$ | $-1/6$ | $\sqrt{6/5}$ | $\sqrt{3}/4$ |
| | $[4]_X[31]_{FS}[31]_F[22]_S$ | $-1/6$ | $\sqrt{6/5}$ | $\sqrt{3}/4$ |
| (iv) $[4]_X[31]_S$: | | | | |
| | $[4]_X[31]_{FS}[211]_F[31]_S$ | $-1$ | $-\sqrt{6/5}$ | $\sqrt{6}/4$ |
| | $[4]_X[31]_{FS}[22]_F[31]_S$ | $-1$ | $-2/\sqrt{5}$ | 1/2 |
| | $[4]_X[31]_{FS}[31]_F[31]_S$ | $-1$ | $2/\sqrt{10}$ | $-\sqrt{2}/4$ |

the resulting matrix elements are

$$\langle \mu_s^D \rangle_i = \frac{M_p}{3m_s}\left[1 + 2\left\langle \sum_{j=1}^{4} \hat{l}_{jz}\hat{S}_j \right\rangle_i\right] P_{s\bar{s}}^i , \quad (14)$$

where $P_{s\bar{s}}^i$ is the probability of the $i^{th}$ strangeness component in the proton. And for the nondiagonal matrix element $\langle \mu_s^{ND} \rangle$, explicit calculations lead to

$$\langle \mu_s^{ND} \rangle_i = \frac{15^{3/4} M_p C_{35}}{27\omega_5} 16\sqrt{6} \mathcal{C}_{FS}^i A_{3q} A_{s\bar{s}}^i , \quad (15)$$

where $A_{3q}$ and $A_{s\bar{s}}^i$ denote the probability amplitudes of the three-quark and the $i$th strangeness components in the proton, and $\mathcal{C}_{FS}^i$ is the corresponding flavor-spin overlap factor for the $i$th strangeness component. $C_{35}$, common to all different strangeness components, is the overlap between the orbital wave function of the residual three-quark in the strangeness component after $s\bar{s}$ annihilation and that of the three-quark component, and reads

$$C_{35} = \left(\frac{2\omega_3\omega_5}{\omega_3^2 + \omega_5^2}\right)^3 , \quad (16)$$

with $\omega_3$ and $\omega_5$ the harmonic oscillator parameters of three- and five-quark components. Note that the expression for $C_{35}$ above differs by a factor of $[2\omega_3\omega_5/(\omega_3^2 + \omega_5^2)]^{3/2}$ from that introduced in, e.g., Refs. [15,16], due to the proper handling of the center-of-motion in the present work.

(ii) $[31]_X$ and $[31]_S$: The total spin of the four-quark subsystem is 1, combined to the orbital angular momentum $L_{[31]_X} = 1$, the total angular momentum of the four-quark subsystem can be $J = 0, 1, 2$, and to form the proton spin 1/2, only the former two are possible alternatives. In the present case, we take the lowest one $J = 0$. Accordingly, the four-quark subsystem cannot contribute to $\mu_s$, and the resulting matrix elements are

$$\langle \mu_s^D \rangle_i = -\frac{M_p}{m_s} P_{s\bar{s}}^i , \quad (17)$$

$$\langle \mu_s^{ND} \rangle_i = -\frac{15^{3/4} M_p C_{35}}{27\omega_5} 16\sqrt{3} \mathcal{C}_{FS} A_{3q} A_{s\bar{s}}^i , \quad (18)$$

(iii) $[4]_X$ and $[22]_S$: Given that the total angular momentum of the four-quark subsystem is 0, it does not contribute to $\mu_s$. Consequently, once we remove the contributions of the momentum of the proton center-of-mass motion, we obtain the following matrix elements:

$$\langle \mu_s^D \rangle_i = -\frac{M_p}{m_s}\left(\frac{1}{5} - \frac{2}{15}\left\langle \sum_{j=1}^{4} \hat{S}_j \right\rangle_i\right) P_{s\bar{s}}^i , \quad (19)$$

$$\langle \mu_s^{ND} \rangle_i = \frac{15^{3/4} M_p C_{35}}{9\omega_5} 16\sqrt{\frac{2}{5}} \mathcal{C}_{FS}^i A_{3q} A_{s\bar{s}}^i . \quad (20)$$

(iv) $[4]_X$ and $[31]_S$: The total spin of the four-quark subsystem should be $S_{[31]} = 1$, here we assume that the combination of $S_{[31]}$ with orbital angular momentum of the antiquark leads to $J = S_4 \oplus L_{\bar{q}} = 0$, then matrix elements read

$$\langle \hat{\mu}_s^D \rangle_i = -\frac{M_p}{m_s} P_{s\bar{s}}^i , \quad (21)$$

$$\langle \mu_s^{ND} \rangle_i = -\frac{15^{3/4} M_p C_{35}}{9\omega_5} 16\sqrt{\frac{1}{5}} \mathcal{C}_{FS}^i A_{3q} A_{s\bar{s}}^i . \quad (22)$$

Accordingly, explicit calculations of the matrix elements $\langle \sum_{j=1}^4 \hat{l}_{jz}\hat{S}_j \rangle_i$, $\langle \sum_{j=1}^4 \hat{S}_j \rangle_i$, and $\mathcal{C}_{FS}^i$ lead to the results shown in Table I.

## III. NUMERICAL RESULTS AND DISCUSSION

As already mentioned, numerical results reported here were obtained using input parameters (Table II) taken from the literature, as commented below.

For the mass of the strange quark $m_s$ and the mass difference between constituent strange and light quarks $\delta m = m_s - m$, we adopted the commonly used values [40]. The energy shared by five configurations between quarks $E_0$, in the absence of hyperfine interaction, and the term due to the transition between three- and five-quark components ($V$) are taken from our previous work [39], which allowed reproducing the experimental data for the proton flavor asymmetry $\bar{d} - \bar{u}$. The matrix elements of the flavor operators, are linear combinations of the spatial matrix elements, $A_i$, $B_i$, and $C_i$, $i = 0, 1$; the numerical values of which were fixed to those determined in Ref. [40].

The last two parameters in Table II are the harmonic oscillator parameters, $\omega_3$ and $\omega_5$, for the three- and five-quark components, respectively, in baryons. The parameter $\omega_3$ can be inferred from the empirical radius of the proton via $\omega_3 = 1/\sqrt{\langle r^2 \rangle}$, which yields $\omega_3 \simeq 246$ MeV for $\sqrt{\langle r^2 \rangle} = 1$ fm. However, the value of $\omega_5$ is rather difficult to determine empirically. As discussed in Ref. [41], the ratio

$$R = \frac{\omega_5}{\omega_3} , \quad (23)$$

can be larger or smaller than 1. Consequently, we used two sets for $R$ to get the numerical results,

TABLE II. Input parameters (in MeV).

| Parameter | Value | Reference |
|---|---|---|
| $m_s$ | 460 | [40] |
| $\delta m$ | 120 | [40] |
| $E_0$ | 2127 | [35] |
| $V$ | $570 \pm 46$ | [35] |
| $A_0$ | 29 | [40] |
| $B_0$ | 20 | [40] |
| $C_0$ | 14 | [40] |
| $A_1$ | 45 | [40] |
| $B_1$ | 30 | [40] |
| $C_1$ | 20 | [40] |
| $\omega_3$ | 246 & 340 | [34,35,41] |
| $\omega_5$ | 225 & 600 | [34,35,41] |

**Set I:** $\omega_3 = 246$ MeV and $R = \sqrt{5/6} \simeq 0.91$ from setting the confinement strength of three- and five-quark configurations to be the same value [41], leading to $\omega_5 \simeq 225$ MeV and $C_{35} \simeq 0.99$.

**Set II:** $\omega_3 = 340$ MeV and $\omega_5 = 600$ MeV, values adopted to reproduce the data for electromagnetic and strong decays of several baryon resonances [34,35], corresponding to $R \simeq 1.76$ and $C_{35} \simeq 0.63$.

Finally, a crucial ingredient of our approach is the probability of the strange quark-antiquark components $P_{s\bar{s}}$, which is often left as free parameter. Here, we calculated it within the $^3P_0$ formalism [36–38]. Then, that probability turns out [35] to be $P_{s\bar{s}} = 5.7 \pm 0.6\%$, for $V = 570 \pm 46$ MeV.

In the following two subsections we report our results for the strangeness magnetic moment $\mu_s$ and magnetic form factor $G_M^s$ of the proton and compare them with the latest data and few most recent/relevant theoretical investigations.

### A. Strangeness magnetic moment of the proton

Our results for diagonal and nondiagonal components of $\mu_s$ are reported in Table III, for the central value $V = 570$ MeV and the two Sets with respect to the $[R, \omega_3, \omega_5]$ ensembles presented above.

In Table III the first column shows the four categories and the second one the associated configurations. Accordingly, contributions from each one of the twelve configurations are reported. Probability amplitudes, calculates within the $^3P_0$ model are depicted in the third column. The fourth column gives the relative weight for each configuration in $P_{s\bar{s}} = 5.7\%$. The diagonal terms (fifth column), not depending on $\omega_5$, are identical for the two sets. Finally, the last two columns correspond to the contributions from nondiagonal terms for Sets I and II, respectively. Several features deserve comments, which will also be useful in shedding light on the results from other sources.

$A^i_{s\bar{s}}$: The probability amplitudes for all $[31]_X$ configurations are negative, except for the one with flavor-spin wave function $[31]_{FS}[31]_F[31]_S$, while those for configurations with $[4]_X$ are positive, except for the $[31]_{FS}[31]_F[31]_S$ configuration.

$P^i_{s\bar{s}}/P^{\rm tot}_{s\bar{s}}$: The total contribution of each category is around $24 \pm 4\%$, so comparable to each other. However, the probabilities of individual configurations span from 1% to 17%.

$\mu_s^D$: The diagonal terms are positive in the first category and negative in the other three. The absolute values from one configuration to another show variations reaching almost one order of magnitude.

$\mu_s^{ND}$: The difference between Sets I and II per configuration is merely due to the different $[\omega_3, \omega_5]$ ensembles used in the present work. Nondiagonal terms have opposite signs with respect to the corresponding diagonal ones in all categories, except the last one. Per configuration, the magnitude of non-diagonal term is larger, in some cases by two orders of magnitudes, than that of the corresponding diagonal term.

$\mu_s^D + \mu_s^{ND}$: Accordingly, the sum of the diagonal and nondiagonal terms per configuration is dominated by far by

TABLE III. Diagonal $\mu_s^D$ and nondiagonal $\mu_s^{ND}$ contributions to the strangeness magnetic moment of the proton from each configuration for Sets I and II, with $A^i_{s\bar{s}}$ the probability amplitude and $P^i_{s\bar{s}}/P^{\rm tot}_{s\bar{s}}$ the relative weight of the strangeness probability in the proton; $P^{\rm tot}_{s\bar{s}} = \sum_{i=1}^{12} P^i_{s\bar{s}}$.

| Category | Configuration | $A^i_{s\bar{s}}$ | $P^i_{s\bar{s}}/P^{\rm tot}_{s\bar{s}}$ (%) | $\mu_s^D$ ($\mu_N$) | Set I $\mu_s^{ND}$ ($\mu_N$) | Set II $\mu_s^{ND}$ ($\mu_N$) |
|---|---|---|---|---|---|---|
| (i) $[31]_X[22]_S$: | | | | | | |
| | $[31]_X[4]_{FS}[22]_F[22]_S$ | −0.099 | 17 | 0.0100 | −1.0043 | −0.2403 |
| | $[31]_X[31]_{FS}[211]_F[22]_S$ | −0.060 | 6 | 0.0040 | −0.6121 | −0.1464 |
| | $[31]_X[31]_{FS}[31]_F[22]_S$ | −0.051 | 5 | 0.0029 | −0.5196 | −0.1243 |
| *Subtotal 1* | | | *28* | *0.0169* | *−2.1360* | *−0.5110* |
| (ii) $[31]_X[31]_S$: | | | | | | |
| | $[31]_X[4]_{FS}[31]_F[31]_S$ | −0.079 | 11 | −0.0128 | 0.8033 | 0.1922 |
| | $[31]_X[31]_{FS}[211]_F[31]_S$ | −0.057 | 6 | −0.0066 | 0.5767 | 0.1380 |
| | $[31]_X[31]_{FS}[22]_F[31]_S$ | −0.042 | 3 | −0.0036 | 0.4273 | 0.1022 |
| | $[31]_X[31]_{FS}[31]_F[31]_S$ | 0.028 | 1 | −0.0016 | 0.1617 | 0.0387 |
| *Subtotal 2* | | | *21* | *−0.0246* | *1.9690* | *0.4711* |
| (iii) $[4]_X[22]_S$: | | | | | | |
| | $[4]_X[31]_{FS}[211]_F[22]_S$ | 0.092 | 15 | −0.0029 | 0.8894 | 0.2128 |
| | $[4]_X[31]_{FS}[31]_F[22]_S$ | 0.081 | 11 | −0.0022 | 0.7772 | 0.1859 |
| *Subtotal 3* | | | *26* | *−0.0051* | *1.6666* | *0.3987* |
| (iv) $[4]_X[31]_S$: | | | | | | |
| | $[4]_X[31]_{FS}[211]_F[31]_S$ | 0.088 | 13 | −0.0157 | −0.8450 | −0.2022 |
| | $[4]_X[31]_{FS}[22]_F[31]_S$ | 0.066 | 8 | −0.0089 | −0.5202 | −0.1244 |
| | $[4]_X[31]_{FS}[31]_F[31]_S$ | −0.044 | 3 | −0.0039 | −0.2426 | −0.0580 |
| *Subtotal 4* | | | *24* | *−0.0285* | *−1.6078* | *−0.3846* |
| | TOTAL | - | 100 | −0.0413 | −0.1082 | −0.0258 |

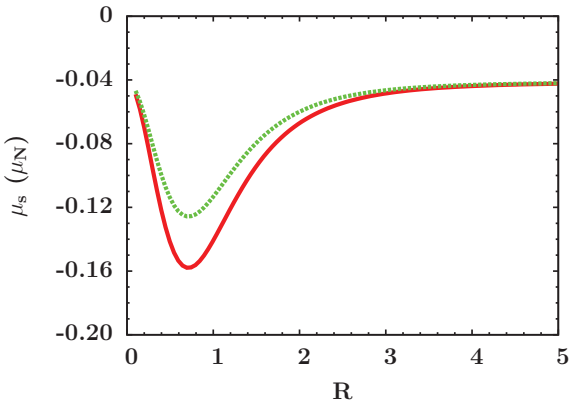


FIG. 1. (Color online) The strangeness magnetic moment of the proton $\mu_s$ in units of nuclear magnetons ($\mu_N$) as a function of the ratio $R = \omega_5/\omega_3$, for $\omega_3 = 246$ MeV (full red curve) and $\omega_3 = 340$ MeV (dotted green curve).

the nondiagonal term. However, it is important to underline the following point: the last line in Table III shows that, due to significant cancelations among the nondiagonal terms from various configurations, the ratio of the sum of nondiagonal terms ($-0.1082$ and $-0.0258$) over that of the diagonal ones ($-0.0413$), is 2.6 (Set I) or 0.6 (Set II), so very significantly different from that ratio per configuration, and even per category.

From the above considerations, we infer an important finding: retaining only the diagonal terms and/or using a configuration truncated scheme will lead to unreliable results, as discussed in Sec. III C.

Finally, using values in the last line of Table III our predictions for the proton strangeness magnetic moment $\mu_s$ are $-0.149 \pm 0.004\mu_N$ for Set I and $-0.067 \pm 0.004\mu_N$ for Set II, with the reported uncertainties corresponding to the range $V = 570 \pm 46$ MeV [35].

It is worth to underline two features: both sets lead to small and negative values for $\mu_s$, though the two results differ one from another by more than $20\sigma$. This latter observation shows the high sensitivity of the strangeness magnetic moment to the ratio $R = \omega_5/\omega_3$.

In Fig. 1 $\mu_s$ is depicted as a function of $R$, varying from 0.1 to 5, corresponding to the size of the strangeness component going from 10 to 0.2 times that of the three-quark configuration, with $\omega_3$ fixed at 246 MeV (full curve) and at 340 MeV (dotted curve). The maximum discrepancy between the two curves is roughly 20% at the minimum values for $\mu_s$, located at $R \simeq 0.71$. So, $\mu_s$ depends mildly on the exact value of $\omega_3$, but strongly on that of $\omega_5$ and hence $R$. The proton strangeness magnetic moment turns out then to be significantly sensitive to that ratio in the range $0.1 < R < 3$, where $\mu_s$ varies by a factor of 4. In any case, according to our study, $\mu_s$ is small and negative.

### B. Strangeness magnetic form factor of the proton

In order to extend the present approach to the $Q^2$-dependent strangeness magnetic form factor of the proton $G_M^s$, for which experimental data are available, we need to calculate the matrix elements of the transitions $\langle uuds\bar{s}|\vec{J}|uuds\bar{s}\rangle$ and $\langle uud|\vec{J}|uuds\bar{s}\rangle$ for both diagonal and nondiagonal terms. For the former ones, explicit calculations lead to

$$\left(G_M^s\right)^D = \mu_s^D e^{-q^2/(5\omega_5^2)}, \tag{24}$$

except for two of the configurations with four-quark subsystem wave functions being $[4]_X[31]_{FS}[211]_F[22]_S$ and $[4]_X[31]_{FS}[31]_F[22]_S$, for which the expression reads

$$\left(G_M^s\right)^D = \left(\mu_s^D - \frac{2q^2}{15\omega_5^2}\right) e^{-q^2/(5\omega_5^2)}. \tag{25}$$

For the nondiagonal transitions between all the strangeness configurations and the three-quark component of the proton, the strangeness magnetic form factor is

$$\left(G_M^s\right)^{ND} = \mu_s^{ND} e^{-4q^2/(15\omega_5^2)}, \tag{26}$$

with the photon three-momentum term ($q^2$) related to the four-momentum transfer $Q = \sqrt{-k_\gamma^2}$ as

$$q^2 = Q^2\left(1 + \frac{Q^2}{4M_p^2}\right). \tag{27}$$

Given the status of the data, discussed in the next section, we produce comprehensive numerical results at $Q^2 = 0.22$ and 0.624 $(\mathrm{GeV}/c)^2$. Table IV contains the outcome of our calculations on the proton strangeness magnetic form factor for all 12 configurations and for both Sets I and II, bringing in few comments:

$(G_M^s)_i^D$: Because of the $\omega_5$ dependence of $G_M^s$, the diagonal terms are not identical in Sets I and II, as it was the case for $\mu_s$. The magnitude of this component, per configuration, decreases with $Q^2$ as well as in going from Set II to Set I at a fixed $Q^2$.
$(G_M^s)_i^{ND}$: The magnitude of the nondiagonal terms are larger than those of diagonal ones, and they decrease with $Q^2$ and also in going from Set I to Set II at a fixed $Q^2$.
$(G_M^s)_i^D/(G_M^s)_i^{ND}$: The $Q^2$ dependence of this ratio turns out to be quite different for Sets I and II, as shown in Fig. 2. For Set I, between $Q^2 = 0$ and 1 $(\mathrm{GeV}/c)^2$ the ratio decreases by a factor of more than 3 and above $Q^2 \sim 0.4$ $(\mathrm{GeV}/c)^2$, the diagonal terms become larger than the diagonal ones, while in Set II the nondiagonal terms stand for roughly $37 \pm 2\%$ of the sum of the two terms in the whole shown $Q^2$ range.
Signs: There are no sign changes in diagonal and nondiagonal terms for a given configuration at different $Q^2$s, including $Q^2 = 0$.

In the next section we proceed to comparisons between our results and relevant ones reported in the literature.

### C. Discussion

Table V summarizes our numerical results for the strangeness magnetic moment of the proton and its magnetic form factor at four $Q^2$ values. In Fig. 3 results for $G_M^s$ within

TABLE IV. Diagonal and nondiagonal contributions to the strangeness magnetic form factor of the proton from each configuration for Sets I and II, at momentum transfer values $Q^2 = 0.220$ and 0.624 $(\mathrm{GeV}/c)^2$.

| Category | Configuration | Set I, $Q^2 = 0.220$ | | Set II, $Q^2 = 0.220$ | | Set I, $Q^2 = 0.624$ | | Set II, $Q^2 = 0.624$ | |
|---|---|---|---|---|---|---|---|---|---|
| | | $(G_M^s)_i^D$ | $(G_M^s)_i^{ND}$ | $(G_M^s)_i^D$ | $(G_M^s)_i^{ND}$ | $(G_M^s)_i^D$ | $(G_M^s)_i^{ND}$ | $(G_M^s)_i^D$ | $(G_M^s)_i^{ND}$ |
| (i) $[31]_X[22]_S$: | | | | | | | | | |
| | $[31]_X[4]_{FS}[22]_F[22]_S$ | 0.0039 | −0.2918 | 0.0088 | −0.2021 | 0.0005 | −0.0206 | 0.0066 | −0.1394 |
| | $[31]_X[31]_{FS}[211]_F[22]_S$ | 0.0016 | −0.1778 | 0.0035 | −0.1232 | 0.0002 | −0.0126 | 0.0027 | −0.0850 |
| | $[31]_X[31]_{FS}[31]_F[22]_S$ | 0.0011 | −0.1510 | 0.0025 | −0.1046 | 0.0002 | −0.0107 | 0.0019 | −0.0721 |
| *Subtotal 1* | | *0.0066* | *–0.6206* | *0.0148* | *–0.4299* | *0.0009* | *–0.0439* | *0.0112* | *–0.2965* |
| (ii) $[31]_X[31]_S$: | | | | | | | | | |
| | $[31]_X[4]_{FS}[31]_F[31]_S$ | −0.0051 | 0.2334 | −0.0112 | 0.1616 | −0.0007 | 0.0165 | −0.0085 | 0.1115 |
| | $[31]_X[31]_{FS}[211]_F[31]_S$ | −0.0026 | 0.1675 | −0.0058 | 0.1160 | −0.0004 | 0.0119 | −0.0044 | 0.0801 |
| | $[31]_X[31]_{FS}[22]_F[31]_S$ | −0.0014 | 0.1241 | −0.0032 | 0.0860 | −0.0002 | 0.0088 | −0.0024 | 0.0593 |
| | $[31]_X[31]_{FS}[31]_F[31]_S$ | −0.0006 | 0.0464 | −0.0014 | 0.0325 | −0.0001 | 0.0033 | −0.0010 | 0.0225 |
| *Subtotal 2* | | *–0.0097* | *0.5714* | *–0.0216* | *0.3961* | *–0.0014* | *0.0405* | *–0.0163* | *0.2734* |
| (iii) $[4]_X[22]_S$: | | | | | | | | | |
| | $[4]_X[31]_{FS}[211]_F[22]_S$ | −0.0011 | 0.2584 | −0.0025 | 0.1790 | −0.0002 | 0.0183 | −0.0019 | 0.1235 |
| | $[4]_X[31]_{FS}[31]_F[22]_S$ | −0.0009 | 0.2258 | −0.0019 | 0.1564 | −0.0001 | 0.0160 | −0.0015 | 0.1079 |
| *Subtotal 3* | | *–0.0020* | *0.4842* | *–0.0044* | *0.3354* | *–0.0003* | *0.0343* | *–0.0034* | *0.2314* |
| (iv) $[4]_X[31]_S$: | | | | | | | | | |
| | $[4]_X[31]_{FS}[211]_F[31]_S$ | −0.0062 | −0.2455 | −0.0138 | −0.1700 | −0.0009 | −0.0174 | −0.0104 | −0.1173 |
| | $[4]_X[31]_{FS}[22]_F[31]_S$ | −0.0035 | −0.1511 | −0.0078 | −0.1047 | −0.0005 | −0.0107 | −0.0059 | −0.0722 |
| | $[4]_X[31]_{FS}[31]_F[31]_S$ | −0.0015 | −0.0705 | −0.0034 | −0.0488 | −0.0002 | −0.0050 | −0.0026 | −0.0337 |
| *Subtotal 4* | | *–0.0112* | *–0.4671* | *–0.0250* | *–0.3235* | *–0.0016* | *–0.0331* | *–0.0189* | *–0.2232* |
| | TOTAL | −0.0163 | −0.0321 | −0.0362 | −0.0219 | −0.0024 | −0.0022 | −0.0274 | −0.0149 |

Sets I and II, spanning the range $0 \leqslant Q^2 \leqslant 1$ $(\mathrm{GeV}/c)^2$ are depicted and compared to the HAPPEX [6] and PVA4 [4] data.

The general trend in our results is that the investigated observable is negative with small magnitude. However, Sets I and II behave differently as a function of $Q^2$. Actually, for Set I, the harmonic oscillator parameter $\omega_5 \simeq 225$ MeV, is smaller than $\omega_5 \simeq 600$ MeV in Set II. So due to the exponential $Q^2$ dependence, $G_M^s$ approaches zero faster in Set I than in Set II. In the following we compare our predictions with results from other sources quoted in Table V.

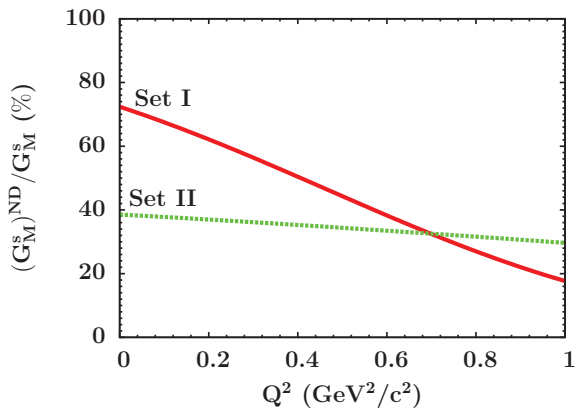


FIG. 2. (Color online) The ratio of nondiagonal to diagonal + nondiagonal terms in the strangeness magnetic form factor of the proton $G_M^s$ as a function of $Q^2$ for Sets I (full red curve) and II (dotted green curve).

At $Q^2 = 0.22$ $(\mathrm{GeV}/c)^2$ both sets give almost identical values, compatible with PVA4 data [4], while at $Q^2 = 0.624$ $(\mathrm{GeV}/c)^2$ Set II is favored by the HAPPEX [6] data. At those two momentum transfer values, data reported by the G0 Collaboration [5] have too large uncertainties to allow informative comparisons with our predictions. To a lesser extent, the same consideration is also true for the SAMPLE Collaboration data [3] at $Q^2 = 0.1$ $(\mathrm{GeV}/c)^2$ with a positive value, large uncertainty and compatible with zero.

In Table V we also show results from lattice-QCD calculations. Quenched QCD complemented by chiral extrapolation techniques performed by Leinweber *et al.* [24] and Wang *et al.* [25] produce for $\mu_s$ and $G_M^s(Q^2 = 0.22)$, respectively, theoretical data compatible with our predictions within less than $2\sigma$ for $\mu_s$ in Set II and $G_M^s$ in both sets. This is also the case for Set II results with respect to the outcome of a $N_f = 2 + 1$ clover fermion LQCD by Doi *et al.* [26] for $\mu_s$ and $G_M^s(Q^2 = 0.10)$, albeit with large uncertainties and smaller, central values in magnitude. Finally, a recent exploratory calculation by Babich *et al.* [27], based on the Wilson gauge and fermion actions on an anisotropic lattice, leads to smaller magnitudes than our predictions at $Q^2 = 0.22$ $(\mathrm{GeV}/c)^2$. While at $Q^2 = 0.62$ $(\mathrm{GeV}/c)^2$ result of the latter work agrees with ours for Set I, at $Q^2 = 0.81$ $(\mathrm{GeV}/c)^2$ Set II produces value compatible with the considered LQCD data.

Here, it is worth mentioning that theoretical predictions as well as recent data (Table V) show (significant) discrepancies with the extracted values from global fits to the data released before 2009: $G_M^s(Q^2 = 0.22) = 0.12 \pm 0.55\mu_N$

TABLE V. Results for the proton strangeness magnetic moment and magnetic form factor (in nuclear magneton) at four $Q^2$ values [in $(\mathrm{GeV}/c)^2$].

| Reference year | Approach | $\mu_s$ | $G_M^s(Q^2=0.10)$ | $G_M^s(Q^2=0.22)$ | $G_M^s(Q^2=0.62)$ | $G_M^s(Q^2=0.81)$ |
|---|---|---|---|---|---|---|
| **Present work: Set I** | $E\chi CQM$ | $-0.149 \pm 0.004$ | $-0.093 \pm 0.002$ | $-0.051 \pm 0.004$ | $-0.006 \pm 0.000$ | $-0.002 \pm 0.000$ |
| **Present work: Set II** | | $-0.067 \pm 0.004$ | $-0.063 \pm 0.004$ | $-0.059 \pm 0.004$ | $-0.045 \pm 0.003$ | $-0.039 \pm 0.003$ |
| Leinweber *et al.* [24] (2005) | LQCD | $-0.046 \pm 0.019$ | | | | |
| Wang *et al.* [25] (2009) | LQCD | | | $-0.034 \pm 0.021$ | | |
| Doi *et al.* [26] (2009) | LQCD | $-0.017 \pm 0.026$ | $-0.015 \pm 0.023$ | | | |
| Babich *et al.* [27] (2012) | LQCD | | | $-0.002 \pm 0.011$ | $-0.007 \pm 0.012$ | $-0.022 \pm 0.016$ |
| Ahmed *et al.* [6] (2012) | Data [HAPPEX] | | | | $-0.070 \pm 0.067$ | |
| Baunack *et al.* [4] (2009) | Data [PVA4] | | | $-0.14 \pm 0.15$ | | |
| Androic *et al.* [5] (2010) | Data [G0] | | | $+0.083 \pm 0.217$ | $-0.123 \pm 0.130$ | |
| Spayde *et al.* [3] (2004) | Data [SAMPLE] | | $+0.37 \pm 0.34$ | | | |

(Ref. [7]), $G_M^s(Q^2=0.21) = 0.19 \pm 0.21\mu_N$. (Ref. [8]), and $G_M^s(Q^2=0.624) = 0.08 \pm 0.11\mu_N$ (Ref. [9]), all of them in disagreement with the latest data from PVA4 [4] and HAPPEX [6] Collaborations.

To end this section, we compare our approach to results coming from similar works [15–17,30,31] reported in the literature.

As mentioned in the Introduction, in Ref. [30] the sign of the proton strangeness magnetic moment was investigated with respect to the strange antiquark states in the five-quark component of the proton. In a subsequent paper [15] the authors calculated $G_M^s(Q^2)$ in the range $0 \leqslant (Q^2) \leqslant 1$ $(\mathrm{GeV}/c)^2$, where data were giving positive values [7–9]. There, two scenarios were adopted (i) $\omega_5 \simeq 2\omega_3$ ($R \simeq 2$) and (ii) $\omega_5 \simeq \omega_3$ ($R \simeq 1$), and also two values for the probability of the $s\bar{s}$, namely $P_{s\bar{s}} = 10\%$ and $15\%$. The three combinations between $R$ and $P_{s\bar{s}}$ studied gave results consistent with the available data in 2006. However, out of the 12 configurations (Table III) only $[31]_X[4]_{FS}[22]_F[22]_S$ was considered. That configuration was also used in Refs. [16,31], where only the diagonal term was included, resulting in $\mu_s = 0.17\mu_N$.

A more recent constituent quark model [17] considered separately only two configurations, namely, $[31]_X[4]_{FS}[22]_F[22]_S$ and $[31]_X[31]_{FS}[211]_F[22]_S$, corresponding to the $\bar{s}$ being in the $S$ or $P$ state, respectively. Pure $P$ state gave $\mu_s = 0.066\mu_N$ and an admixture between the two states $\mu_s = 1.01\mu_N$. In that work, both diagonal and nondiagonal terms were considered for the retained configurations and $\omega_3$ was fixed at 246 MeV, while $\omega_5$ and the probability $P_{s\bar{s}}$ were fitted on the G0 Collaboration [5] data reported in Table V. The extracted values are $\omega_5 = 469$ MeV and $P_{s\bar{s}} = 0.025\%$, smaller by more than two orders of magnitude compared to the $^3P_0$ model result employed in the present work. Using their approach, the authors found that putting $P_{s\bar{s}} = 2.5\%$, as reported in Ref. [42], leads to $\omega_5 = 108$ MeV. The incredibly tiny probability reported in Ref. [17] can easily be understood. As shown in Table IV, contributions from individual configurations $[31]_X[4]_{FS}[22]_F[22]_S$ or $[31]_X[31]_{FS}[211]_F[22]_S$ compared to the total of contributions from all twelve of them differ by up to two orders of magnitude.

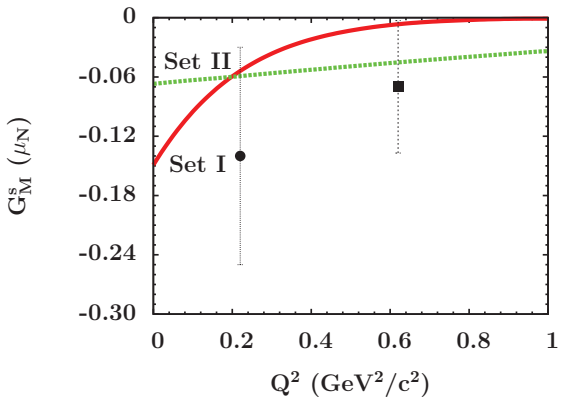


FIG. 3. (Color online) The strangeness magnetic moment of the proton $G_M^s$ as a function of the momentum transfer $Q^2$ for Sets I (full red curve) and II (dotted green curve). Data are from Refs. [4,6].

## IV. SUMMARY AND CONCLUSIONS

The extended chiral constituent quark model offers an appropriate frame to study the possible manifestations of genuine five-quark components in baryons. The present work is in line with our earlier efforts [34,35,39] in that realm. There are several difficulties in this endeavor: few observables have been identified carrying information on higher Fock states, the data are scarce and often bear large uncertainties due to the smallness of the effects looked for. Moreover, there are input parameters in the approach, which basically should be taken from literature and exceptionally fitted on the data under consideration. Accordingly, we took advantage of the data on radiative and strong decays of the $\Lambda(1405)$ resonance [34], strong decay of low-lying $S_{11}$ and $D_{13}$ nucleon resonances [35], and sea flavor content of octet baryons [39] to deepen our understanding of the five-quark components and select a coherent set of input parameters.

Our main findings can be summarized in three points, as follows:

(i) Five-quark Fock states: we gave detailed numerical results for both diagonal and nondiagonal terms for all of the 12 relevant configurations showing strong interplays among different components with (very) large cancellations.

(ii) Probability of the $s\bar{s}$ in the proton wave function: we determined $P_{s\bar{s}}$ using a $^3P_0$ pair creation model, as in a previous work [39].

(iii) Harmonic oscillator parameters: it was shown that with respect to the parameters $\omega_3$ and $\omega_5$, the important element is the ratio $R = \omega_5/\omega_3$.

Based on the above observations, it then becomes obvious that using severely truncated configuration sets and/or unrealistic values for $P_{s\bar{s}}$ or $R$ will lead to unreliable results with respect to the magnetic moment and/or magnetic form factor of the proton.

In the present paper we showed that our predictions are in reasonable agreement with recent measurements [4,6] and lattice-QCD results [24–27]. The uncertainties associated to the available data on the one hand, and those of LQCD approaches on the other hand, do not allow us to make a sharp choice between the results coming from the two sets in terms of the ratio $R$. It is nevertheless clear that the strangeness magnetic moment of the proton and its magnetic form factor are small and negative. Between the two sets, Set II appears to be slightly favored by findings from other sources. Accordingly, we get $\mu_s = -0.0670 \pm 0.004\mu_N$ and the magnitude of the strangeness magnetic from factor of the proton evolves smoothly with increasing transfer momentum to reach $G_M^s(Q^2) = -0.033 \pm 0.003\mu_N$ at $Q^2 = 1\ (\mathrm{GeV}/c)^2$.

Awaited-for data at $Q^2 = 0.6\ (\mathrm{GeV}/c)^2$ expected to be released by the PVA4 Collaboration [4] and more advanced LQCD approaches will hopefully improve the accuracy of the experimental and theoretical data bases. Recent convergence between theory and experiment on the negative sign of that observable and its smallness, might also initiate new dedicated measurements.

## ACKNOWLEDGMENTS

We wish to thank the anonymous referee for his/her careful reading of the manuscript. This work was supported by the National Natural Science Foundation of China under Grant No. 11205164.

[1] D. S. Armstrong and R. D. McKeown, Ann. Rev. Nucl. Part. Sci. **62**, 337 (2012).
[2] R. Gonzalez-Jimenez, J. A. Caballero, and T. W. Donnelly, Phys. Rep. **524**, 1 (2013).
[3] D. T. Spayde *et al.* (SAMPLE Collaboration), Phys. Lett. B **583**, 79 (2004).
[4] S. Baunack *et al.* (PVA4 Collaboration), Phys. Rev. Lett. **102**, 151803 (2009).
[5] D. Androic *et al.* (G0 Collaboration), Phys. Rev. Lett. **104**, 012001 (2010).
[6] Z. Ahmed *et al.* (HAPPEX Collaboration), Phys. Rev. Lett. **108**, 102001 (2012).
[7] R. D. Young, J. Roche, R. D. Carlini, and A. W. Thomas, Phys. Rev. Lett. **97**, 102002 (2006).
[8] J. Liu, R. D. McKeown, and M. J. Ramsey-Musolf, Phys. Rev. C **76**, 025202 (2007).
[9] S. F. Pate, D. W. McKee, and V. Papavassiliou, Phys. Rev. C **78**, 015207 (2008).
[10] T. R. Hemmert, U.-G. Meißner, and S. Steininger, Phys. Lett. B **437**, 184 (1998).
[11] T. R. Hemmert, B. Kubis, and Ulf-G. Meißner, Phys. Rev. C **60**, 045501 (1999).
[12] R. Lewis, W. Wilcox, and R. M. Woloshyn, Phys. Rev. D **67**, 013003 (2003).
[13] A. Silva, H.-C. Kim, and K. Goeke, Eur. Phys. J. A **22**, 481 (2004).
[14] Z.-T. Xia and W. Zuo, Phys. Rev. C **78**, 015209 (2008).
[15] D. O. Riska and B. S. Zou, Phys. Lett. B **636**, 265 (2006).
[16] C. S. An, Q. B. Li, D. O. Riska, and B. S. Zou, Phys. Rev. C **74**, 055205 (2006); **75**, 069901(E) (2007).
[17] A. Kiswandhi, H.-C. Lee, and S.-N. Yang, Phys. Lett. B **704**, 373 (2011).
[18] H. Forkel, F. S. Navarra, and M. Nielsen, Phys. Rev. C **61**, 055206 (2000).
[19] X.-S. Chen, R. G. E. Timmermans, W.-M. Sun, H.-S. Zong, and F. Wang, Phys. Rev. C **70**, 015201 (2004).
[20] L. Hannelius and D. O. Riska, Phys. Rev. C **62**, 045204 (2000).
[21] V. E. Lyubovitskij, P. Wang, T. Gutsche, and A. Faessler, Phys. Rev. C **66**, 055204 (2002).
[22] R. Bijker, J. Ferretti, and E. Santopinto, Phys. Rev. C **85**, 035204 (2012).
[23] D. B. Leinweber and A. W. Thomas, Phys. Rev. D **62**, 074505 (2000).
[24] D. B. Leinweber *et al.*, Phys. Rev. Lett. **94**, 212001 (2005).
[25] P. Wang, D. B. Leinweber, A. W. Thomas, and R. D. Young, Phys. Rev. C **79**, 065202 (2009).
[26] T. Doi, M. Deka, S.-J. Dong, T. Draper, K.-F. Liu, D. Mankame, N. Mathur, and T. Streuer, Phys. Rev. D **80**, 094503 (2009).
[27] R. Babich, R. C. Brower, M. A. Clark, G. T. Fleming, J. C. Osborn, C. Rebbi, and D. Schaich, Phys. Rev. D **85**, 054510 (2012).
[28] D. H. Beck and R. D. McKeown, Ann. Rev. Nucl. Part. Sci. **51**, 189 (2001).
[29] E. J. Beise, M. L. Pitt, and D. T. Spayde, Prog. Part. Nucl. Phys. **54**, 289 (2005).
[30] B. S. Zou and D. O. Riska, Phys. Rev. Lett. **95**, 072001 (2005).
[31] C. S. An, D. O. Riska, and B. S. Zou, Phys. Rev. C **73**, 035207 (2006).
[32] Q. B. Li and D. O. Riska, Phys. Rev. C **73**, 035201 (2006).
[33] Q. B. Li and D. O. Riska, Phys. Rev. C **74**, 015202 (2006).
[34] C. S. An, B. Saghai, S. G. Yuan, and J. He, Phys. Rev. C **81**, 045203 (2010).
[35] C. S. An and B. Saghai, Phys. Rev. C **84**, 045204 (2011).
[36] A. Le Yaouanc, L. Oliver, O. Pene, and J. C. Raynal, Phys. Rev. D **8**, 2223 (1973).
[37] A. Le Yaouanc, L. Oliver, O. Pene, and J. C. Raynal, Phys. Rev. D **9**, 1415 (1974).
[38] R. Kokoski and N. Isgur, Phys. Rev. D **35**, 907 (1987).
[39] C. S. An and B. Saghai, Phys. Rev. C **85**, 055203 (2012).
[40] L. Ya Glozman and D. O. Riska, Phys. Rep. **268**, 263 (1996).
[41] C. S. An, B. Ch. Metsch, and B. S. Zou, Phys. Rev. C **87**, 065207 (2013).
[42] W.-C. Chang and J.-C. Peng, Phys. Rev. Lett. **106**, 252002 (2011).